Power Consumption and Gas Capacity of Self-inducting Turbo Aerators

YURY ZUNDELEVICH

Materials and Molecular Research
Division of Lawrence Berkeley Laboratory
and
Department of Materials Science and
Mineral Engineering
University of California at Berkeley
Berkeley, California 94720

A theoretical and experimental analysis of self-inducting turbo aerator performance was carried out based on the theory of water jet injector operation. It was shown that the aerator's injection coefficient is completely determined by only two dimensionless groups, C_H and Eu_G, between which there is a single valued dependence on whose basis generalization of experimental data is possible. An analytical expression for the optimality criterion or aerator performance index, accounting for aerator gas capacity, power consumption, and submergence, has been obtained in terms of C_H and Eu_G with only one adjustable parameter. From the above two dependencies, a methodology was developed for determining optimal operating conditions, by means of which all the data necessary for the optimal design can be obtained from the results of bench scale experiment.

SCOPE

Gas-liquid contacting systems have found a wide range of applications; they are encountered in such industrial processes as autoclave leaching of ores and concentrates, flotation of ores, coals and concentrates, wastewater treatment by activated sludge, and aerobic fermentation.

No matter whether the gas is consumed by chemical reaction or serves just as a carrier for the solids (as in flotation processes), the overall efficiency of such processes substantially depends upon the total gas-liquid interfacial area. Consequently, it is usual to carry out these processes in mechanically stirred tanks equipped with gas spargers and impellers (henceforth gas sparged tanks) or with self-inducting impeller aerator alone (henceforth tanks with self-inducting aerators). Because gas to liquid mass transfer often can be the rate limiting step in gas-liquid reactor performance, a considerable number of studies concerned with correlations between the overall volumetric mass transfer coefficient and mechanical agitation power per unit volume have been carried out (Calderbank, 1958, 1959; Calderbank and Moo-Young, 1961; Lee and Meyrick, 1970; Robinson and Wilke, 1973). Some investigators provided correlations between mechanical power requirement and gas holdup using different dimensionless groups, such as aeration number $N_A = Q/ND^3$ or impeller Weber Number $N_{We} = N^2D^3\rho/\sigma$ for gas sparged tanks (Ohyama and Endoh, 1955; Michel and Miller, 1962; Blakebrough and Sambamurthy, 1964; Hassan and Robinson, 1977). The situation with self-inducting aerators, widely used in hydrometallurgy and flotation, is somewhat different. The available data are basically descriptive in their nature and do not lend themselves to the needs of design and/or modeling of such devices (Mitrofanov, 1959; Klassen, 1949, 1954; Medvedev 1955, 1957; Arbiter et al., 1968). There are, however, a number of studies dealing with experimental testing of self-inducting aerators in flotation processes where they were employed earlier than their use in autoclave processes. In the former application, these aerators are very effective (Medvedev, 1955, 1959; Mitrofanov, 1959).

The use of self-inducting aerators affords a number of advantages over gas sparging, such as less power consumption and better dispersion (Zaytsev, 1973) and, even more significantly, flexibility due to their ability to recirculate gas. For instance, in systems in which oxygen is contacted with aqueous solutions, due to limited oxygen solubility in water and aqueous solutions, sufficiently high levels of oxygen utilization can be reached only by manifold passage of the gas bubbles through the liquid. Owing to lack of the previous investigations and great variety of different self-inducting aeration devices, some restrictions on the scope of this seemed to be necessary. The present study provides a theoretical and experimental analysis of a self-induction turbo aerator (see Figure 2) which was found to be the most efficient device in comparison with other types (Zundelevich, 1975). The research objective was to design a modeling method suitable for this device. Such a method would allow the design of industrial aerators from the results of bench or pilot scale experiments. This approach seemed to be more appropriate than an attempt to develop a direct computational procedure in view of the complexity inherent in the gas aspiration process of self-inducting turbo aerator.

Several design versions within this aerator type (Figure 2) with 0.1 m rotor were used in experiments. Additionally, three geometrically similar aerators with rotor diameters respectively 0.08, 0.1, and 0.12 m were studied. A transparent cylindrical baffled 0.4 m tank filled with 50×10^{-3} m^3 of water has been used throughout the experiments. The aerator gas capacity, impeller rotational speed, and power input have been measured over ranges from 0.1×10^{-3} to 5.5×10^{-3} m^3/s, 6 to 40 s^{-1}, and 30 to 1 500 W, respectively, for the aerator submergence over range from 0.5 to 2.0 m.

The study was limited mainly to the prediction of such characteristics as power consumption P and aerator gas capacity Q_G (and their optimal combination) rather than prediction of gas-liquid mass transfer coefficient, which was the objective of many previous investigators. However, the theoretical development of this study makes it possible to consider a number of scale-up versions concerned with mass transfer problems.

0001-1541-79-2744-0762-$01.25.

CONCLUSIONS AND SIGNIFICANCE

Theoretical analysis and experimental observations lead to the conclusion that the gas aspiration mechanism of the aerator in question is mainly an injectional one. By analysis of the expression for the injection coefficient of regular water jet injectors, obtained by Sokolov and Zinger (1960), it was established that the gas capacity of self-inducting turbo aerators does not depend on liquid phase density. Furthermore, the gas capacity is determined only by the aerator's pumping capacity with respect to liquid (ηND^3), rotor tip speed (πDN), and the value of submergence (H), enabling the generalization of the experimental data on the basis of a single valued dependence between two dimensionless groups $C_H \equiv gH/(ND)^2$ and $Eu_G \equiv gH/(Q_G/D^2)^2$. In addition, it was established that aerator gas capacity Q_G and power consumption P are both proportional to the second power of rotor diameter for geometrically similar aerators, provided rotor tip speed and submergence are constant. Therefore, the ratio Q_G/P (specific capacity) is also constant under the above conditions. The specific capacity was found to be inversely proportional to the aerator submergence at constant value of C_H, which means that aerator performance index Q_GH/P in turn is a constant value for the aerators of the same design and for the same gas-liquid system. Particularly, the maximum value of Q_GH/P found for the bench scale aerator will remain the same for any geometrically similar industrial aerator provided C_H is the same on both scales. An analytical equation for aerator performance index in terms of C_H and Eu_G with only one adjustable parameter (η) was obtained, enabling the use of the generalized experimental dependence of Eu_G on C_H for calculation and optimization of aerator performance under industrial conditions. The analytical expression for Q_GH/P derived from theoretical considerations is in good agreement with the experimental data. It contains no tank geometry terms, which means that aerator performance at constant submergence is essentially the same in tanks of different geometry and volume. Consequently, no full geometrical similarity is required for self-inducting aerator modeling and scale-up.

PREVIOUS WORK

Several decades ago, self-inducting aerators were brought into use in flotation and a little later in hydrometallurgical processes. They also can be utilized in biological wastewater treatment and biochemical as well as some chemical processes. Although self-inducting aerators are commonly used, the number of publications concerned with these devices remains relatively limited.

Quite a few different types of self-inducting impellers have been designed, the simplest of which resembles a hollow shaft with a T shaped lower part (see, for example, Joshi and Sharma, 1977). The ends of the T have orifices or are cut off obliquely, and rotation in the liquid causes suction at these ends. Consequently, gas passes down the shaft to the T and thence into the liquid. Among the shortcomings of this impeller type are low specific gas capacity and poor dispersion ability.

More complicated aerator designs usually consist of stator and rotor. They may be divided into two principal types. The first (Figure 1) has a rotor consisting of a solid disk with radial blades fixed on top of it. The shaft on which this rotor is mounted is within a standpipe which ends with a stator shaped as a disk with vertical blades fixed underneath it and positioned at an angle to the radius. Apertures in the stator disk or the hollow tube are provided for circulation of liquid. The flow of circulating liquid is ejected radially by the revolving rotor together with the ejected gas incoming through the standpipe.

The second type of aerator (Figure 2) has a rotor consisting of a central solid disk with radial blades mounted at its periphery, the blades being enclosed on top and underneath by hollow disks. The stator is similar to that of the first type of aerator except that the stator blades are enclosed on both the top and bottom by hollow disks. The standpipe and the stator usually do not have apertures for circulation of liquid. The central solid disk divides the rotor's cavity into two zones. The lower zone is for circulation of liquid sucked vertically upward through the central opening of the lower hollow disk and later ejected together with the ejected gas incoming to the upper zone through the standpipe and the central opening of the upper hollow disk. Within each of those two types of aerators, there are numerous constructional modifications.

Most of the constructional modifications of the aerators described in the literature are reduced to one of the above two versions. However, numerous attempts at developing a theory of aerator behavior or at least an adequate method of generalizing experimental data have not yet been successful. It is appropriate to mention the excellent survey by Harris (1976) containing 131 references and giving an adequate account of the field at that time. "Empiricism and rule-of-thumb have guided flotation machine design and scale-up, and a current need is for the development of a fundamental understanding of the subject."

Indeed, there is not even agreement concerning the mechanism of gas aspiration by impellers. Some investigators (Rundkvist, 1963; Medvedev, 1955; Medeved and Shestakov, 1957) are inclined to consider an aerator with stator as a low head centrifugal pump performing under conditions atypical for a centrifugal pump. The equation for the theoretical head of an aerator as a function of liquid and air capacity suggested by Medvedev (1955) by an analogy with a well-known equation for the theoretical head of a centrifugal pump was not verified experimentally.

The principles of modeling self-inducting impellers, based on aerator characteristic curves of the same type as those for centrifugal pumps, were suggested by Mitrofanov (1959). This approach was unsuccessful owing to the absence of stable pump characteristics for a high percentage of air in air-water mixtures (centrifugal pumps normally inoperable above 10 to 15% air).

It was suggested (Kashkarov, 1956) that one considers the aerator as a centrifugal compressor which forces the air into the liquid phase; however, the head created by compressors of such design is too low to overcome the counterpressure of significant liquid depths.

One of the attempts to calculate the performance of self-inducting aerators of the first type (Figure 1) was

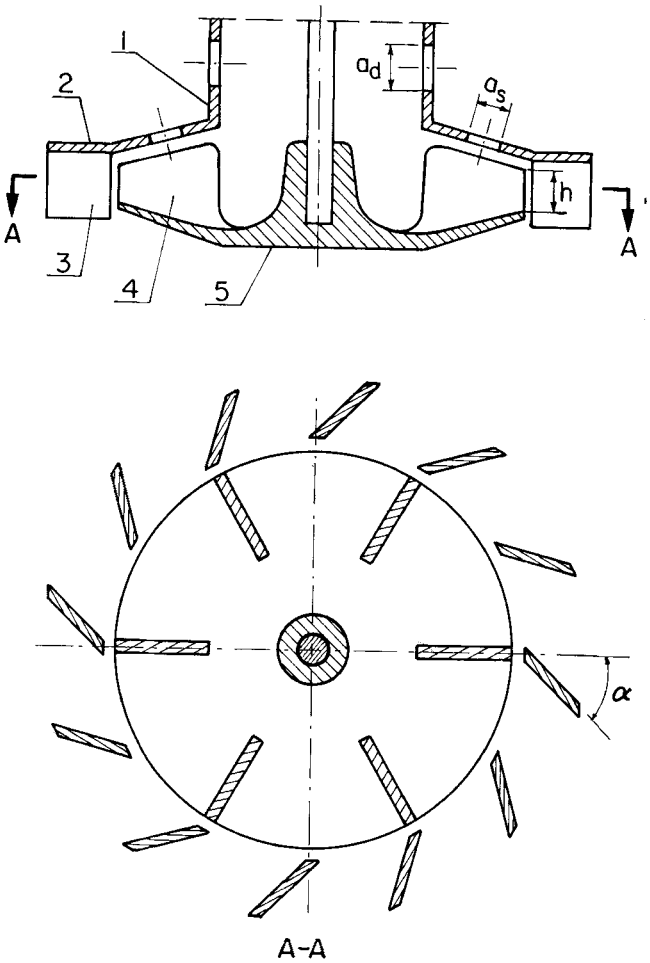

Fig. 1. Self-inducting aerator principle design (type 1): (1) standpipe, (2) stator, (3) stator blades, (4) rotor blades, (5) rotor.

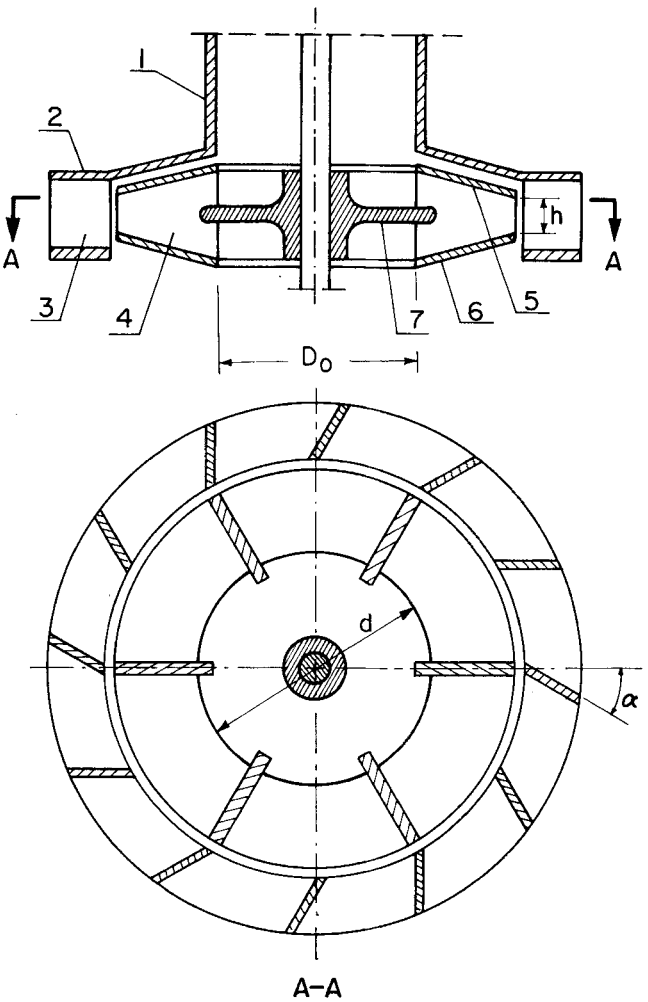

Fig. 2. Self-inducting aerator principle design (type 2): (1) standpipe, (2) stator, (3) stator blades, (4) rotor blades, (5) upper hollow disk, (6) lower hollow disk, (7) central disk.

undertaken by Braginsky (1964). Assuming that the liquid velocity in the stator is small compared to the rotor tip speed, then the static head p_S practically equals the full head of the rotor $K_1\rho\,(\pi DN)^2/2$. Braginsky wrote down the condition of the gas intake into the liquid on the basis of equality of the static head p_S to hydrostatic pressure $p_H = \rho\, gH$ at the outlet from the stator: $p_S = p_H$. Hence, the critical impeller speed N_{cr} at which air aspiration begins is

$$N_{cr} = \sqrt{\frac{2gH}{K_1\pi^2D^2}} \qquad (1)$$

Equation (1) was experimentally verified. However, the expression for gas capacity at $N > N_{cr}$, derived in the same work, turns out to be inconsistent with some experimental data. According to Braginsky (1964), gas capacity Q_G is proportional to the head, developed by rotor $Q_G \propto N^2D^2$, and Q_G increases without limit with the increase of circulation apertures in the stator. In reality, Q_G passes through a maximum at some aperture cross-section area (Rundkvist, 1964), and an experimental plot for Q_G against N is close to a linear one. [The dependence of Q_G on N becomes weaker at high N (Samsonova et al., 1970).]

The complex character of the phenomena determining the mechanism of gas aspiration by an aerator can be illustrated not only by the above example but also by the contradictory results of others. Thus, according to Mitrofanov (1959), Q_G is proportional to the impeller blade width h, although the experiments of the other investigators cited earlier did not show such a dependence.

Industrial and pilot scale tests of both aerator types (Figures 1 and 2) are described in the works of Samsonova et al. (1970) and Zaytsev (1973). The common conclusion of these works is that for the same conditions the gas capacity of the second type of aerator is 2 to 2.5 as high as that for the first type. However, it is likely that the optimal conditions are different and should be specified for each aerator type to achieve the maximum efficiency. The aperture's existence for slurry circulation in the first aerator type of stator (Figure 1) which allows one to tune up the aerator for the given submergence in flotation machines is one evidence of this point. Consequently, the modeling or scale-up step should be preceded by a sufficiently general study in order to establish optimal aerator design and operating conditions. The study of this kind was carried out by Zundelevich (1975). It supports the published viewpoint that for aerators of the second type, the specific gas capacity Q_G/P is two to three times as high as for the first type, especially for a great submergence.

A considerable number of experiments to search for the optimal aerator design (second type) was carried out under Zaytsev (1973). One of the conclusions of that study was that the optimal condition of gas dispersion by the aerator was realized in the self-inducting regime. It was shown that forced supply of additional gas through the standpipe of the aerator did not result in increasing mass transfer between gas and liquid phases. On the

other hand, the visual observation of gas dispersion process in the present work has shown that although extremely fine gas bubble breaking takes place inside the aerator, the bubbles instantly coalesce and leave the stator with a diameter of 2 to 3 mm. The latter size is a stable one for the given gas-liquid system and, at least in water, is insensitive to power input. It implies, therefore, that increase in the mass transfer rate is achieved at the expense of the aerator gas capacity growth rather than stirring itself, although no mass transfer experiments were carried out in the present study.

THEORY

As mentioned earlier, two main types of aerator devices are presently in wide use (Figures 1 and 2). According to the literature (Samsonova et al., 1970; Zaytsev, 1973), superior performance results from use of the second type of aerator. Henceforth, only the closed type of turbine aerators with the central disk (Figure 2) will be considered.

The gas aspiration process of self-inducting aerators is a complicated one and is not yet completely understood. Among the many speculations on the aspiration mechanism, the most likely seems the supposition of injectional mechanism (Samsonova et al., 1970; Zaytsev, 1973). However, there has been no attempt to apply the theory developed for water jet injectors to self-inducting aerators, probably because of the difficulty in recognizing the geometrical elements of the former in the aerator design.

If an aerator is considered as a liquid-gas injector, in which the liquid serves as the driving medium entraining the gas, then its gas capacity should be determined by the relationship

$$Q_G = \Psi Q_L \tag{2}$$

For the water jet injectors, injection coefficient Ψ can be calculated by the equation (Sokolov and Zinger, 1960)

$$\Psi = \sqrt{\frac{K - \dfrac{\Delta p_M}{\Delta p_N}\dfrac{S_M}{S_N}\dfrac{\zeta_3}{2\zeta_1}}{\left(1 - \dfrac{\zeta_3}{2\zeta_1}\right)\dfrac{S_N}{S_M}} - 1} \tag{3}$$

The numerical constant $K = 0.834$ and $\zeta_3/2\zeta_1 = 0.47$ served as adjustable parameters and were defined by Sokolov and Zinger from the results of experiments with an injector schematically depicted in Figure 3.

During liquid-gas ejector operation, the driving medium (water) under pressure p_N moves out of the nozzle and aspirates gas, which comes into the reception chamber under pressure p_0 (Figure 3). As both liquid and gas streams move away from the nozzle through the mixing chamber, their pressures approach each other and at some distance become equal. From the mixing chamber, the gas-liquid dispersion enters the divergent diffuser where its velocity drops and pressure rises to overcome counterpressure p_M of the outer medium at the diffuser outlet.

In principle, the same design elements can be found in the aerator design (Figure 3). Thus, either the gap between lower hollow and central solid disks, where the liquid first contacts gas, or the gap between upper and lower hollow disks at the rotor outlet, where the liquid jet achieves its maximum velocity, could be regarded as corresponding to the nozzle in the injector. The volume between the hollow disks serves also as a mixing chamber and probably as a diffuser because the cross-section area is not constant but rather greater at greater radius. Finally, the entire zone between the stator blades could serve not

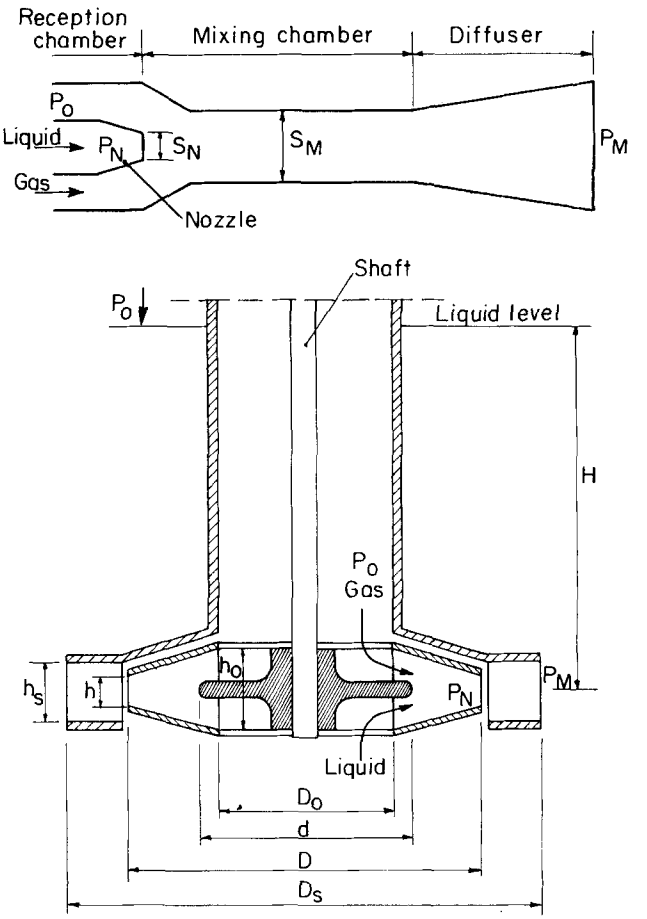

Fig. 3. Comparative geometry of water jet injector (top sketch) and self-inducting aerator (bottom sketch).

only as a diffuser but as a mixing chamber extension in case the distance inside the rotor is not enough to equalize the gas and liquid pressures. It should be recognized that the numerical constants of Equation (3) found for regular liquid-gas ejector are unlikely to apply in the case of the aerator. Nevertheless, the form of Equation (3) should be adequate for aerators due to the similarity of the fundamental principles of gas induction in aerators and ejectors. In this paper, the following areas are defined for use in Equation (3) (Figure 3):

Cross-section area of the nozzle

$$S_N = \pi D \frac{h}{2} \tag{4}$$

Cross-section area of the mixing chamber

$$S_M = \pi D_s h_s \tag{5}$$

One of the optimal design version dictates (Sokolov and Zinger, 1960)

$$D_s = 1.4D \tag{6}$$

and

$$h_s = 2h \tag{7}$$

We assume that gas entering the aerator standpipe (Figure 3) is under the same pressure p_0 as the gas space above liquid surface in the vessel. This corresponds to regular industrial condition. Resistance to gas movement through aerator standpipe as the measurements had shown (Rundkvist, 1963, 1964) does not exceed several millimeters of water. Therefore, the pressure drop in the standpipe is neglected.

The total counterpressure p_M at the aerator level is equal to the sum of the vessel gas space pressure p_0 and the hydrostatic water pressure above the aerator:

$$p_M = \rho gH + p_0 \tag{8}$$

Total pressure of the working liquid p_N is equal to the sum of gas space pressure p_0, hydrostatic pressure ρgH, and total head of the aerator, the lower part of which works as a centrifugal pump:

$$p_N = \rho gH + \rho K_1 \frac{(\pi DN)^2}{2} + p_0 \tag{9}$$

Substitution of Equations (4) to (9) into Equation (3) for the injection coefficient yields

$$\Psi = 3\sqrt{1 - 3\frac{2C_H}{2C_H + K_1\pi^2}} - 1 \tag{10}$$

It is unlikely that Equation (10) can be used for reliable prediction of the injection coefficient owing to lack of the distinctly pronounced injector elements in self-inducting aerator design. What is important, however, is that this equation contains the dimensionless group (henceforth the head coefficient)

$$C_H \equiv \frac{gH}{(ND)^2} \tag{11}$$

which can be regarded as the ratio of the hydrostatic and dynamic heads. Clearly, Ψ is determined by the head coefficient alone. It is also seen from Equations (10) and (11) that injection coefficient does not depend on the liquid phase density ρ.

The aerator gas capacity Q_G from relationship (2) is determined not only by the injection coefficient but also by the volumetric liquid velocity Q_L, that is, by the aerator pumping capacity. The pumping capacity Q_L of any stirrer is defined by the equation (see, for instance, Uhl and Gray, 1966)

$$Q_L = \eta ND^3 \tag{12}$$

where the coefficient η, the dimensionless pumping capacity, depends on the type and design of impeller. For a propeller with the ratio of pitch to diameter equal to 1, the theoretical value of η is equal to $\pi/6$, which is close to the experimentally determined $\eta = 0.5 - 0.59$ (Fort, 1969). For the standard disk turbine with the blade width $h = D/5$, $\eta = 0.7$ to 0.9 according to the experimental data, the lower values being correspondent to the lower D/T ratio (Cooper and Wolf, 1968). On the other hand, Hicks et al. (1976) report the values of η found in the same interval but in reversed dependence on D/T ratio. Analogous data for self-inducting turbo aerators are not available. However, for turbines, η is proportional to the blade width (Cooper and Wolf, 1968), and the aerator blade is about half that of the standard turbine. Furthermore, the liquid is sucked in by only the lower part of the aerator which, in addition, is partially enclosed with the hollow disk. Consequently, the value of η in the aerator case can be expected to be less by about one order of magnitude than for the standard turbine.

Manipulating Equations (10), (2), and (12), we get

$$1 = 3\sqrt{\frac{1}{\Psi^2} - 3\eta^2\frac{2Eu_G}{2C_H + K_1\pi^2}} - \frac{1}{\Psi} \tag{13}$$

where

$$\frac{1}{\Psi} = \frac{\eta ND^3}{Q_G} = \eta\sqrt{\frac{Eu_G}{C_H}} \tag{14}$$

and

$$Eu_G \equiv \frac{gH}{(Q_G/D^2)^2} \tag{15}$$

is another dimensionless group (henceforth the gas Euler number)*, the gas velocity within the aerator being proportional to the ratio Q_G/D^2. Since Equation (13) does not include any other variables than C_H and Eu_G, it follows that there is a single valued dependence between them on whose basis a generalization of experimental data on aerators is possible.

The plot for Eu_G against C_H can be regarded as a generalized model for the particular aerator design, regardless of scale and operation under various conditions, including the optimal ones.

To introduce the optimality criterion Q_G/P into the dependence between C_H and Eu_G, one can use a known expression for impeller power consumption in the turbulent regime (Uhl and Grey, 1966):

$$P = N_p\rho_D N^3 D^5 \tag{16}$$

where power number N_p is a constant for baffled tanks or for turbines operating with stators (Uhl and Grey, 1966). It is also known that for gas sparged tanks, power input cannot be estimated merely by replacing ρ with the volume averaged gas-liquid dispersion density and using the N_p applicable to gas free liquid mixing. In these latter types of dispersion, the apparent value of N_p is less than that estimated from Equation (16) owing to the formation of a gas cavity behind the impeller (Bruijn et al., 1974; Van't Riet et al., 1976) and the reduction in the local density of the gas-liquid dispersion around the impeller (Topiwala and Hamer, 1974; Calderbank, 1958). For the same reason, N_p, depends on the gas sparging rate as well as upon the impeller speed and diameter (Michel and Miller, 1962). Apart from the above case where nothing was known about the dispersion density within the impeller zone, in the case of self-inducting aerators it is automatically guaranteed that all the gas aspirated passes through the aerator rotor zone. For instance, the data on power reduction in the gas inducing type of agitated contactors were successfully correlated with the parameter Q_G/ND^3 (Joshi and Sharma, 1977) although, rigorously speaking, this correlation does not make sense since Q_G is not an independent parameter in tanks with self-inducting aerators.

The gas-liquid dispersion density ρ_D within aerator zone can be obtained from

$$\rho_D = \frac{Q_G\rho_G + Q_L\rho}{Q_G + Q_L} \tag{17}$$

Taking into account that $\rho_G <<< \rho$ and using formula (2), one can get for ρ_D

$$\rho_D = \frac{\rho}{\Psi + 1} \tag{18}$$

If we take a reciprocal of (14), an equation results which can be used to obtain Ψ knowing η

$$\Psi = \frac{1}{\eta}\sqrt{\frac{C_H}{Eu_G}} \tag{19}$$

Rearranging (15), we get

$$Q_G = D^2\sqrt{\frac{gH}{Eu_G}} \tag{20}$$

Rearranging (16) and employing (18), we get

* While the use of the title 'gas Euler numer' for this group is novel, it is justified in that the numerator and denominator have the same dimensions of the usual Euler number.

$$P = N_p \frac{\rho}{\Psi + 1} (ND)^3 D^2 \qquad (21)$$

By dividing Equation (20) by (21), rearranging the equation obtained, and making use of Equation (19), we can write the equation for the specific capacity of aerator:

$$\frac{Q_G}{P} = \frac{\sqrt{\frac{gH}{Eu_G}}\left(\frac{1}{\eta}\sqrt{\frac{C_H}{Eu_G}} + 1\right)}{N_p \rho (ND)^3}$$

$$= \frac{\sqrt{\frac{C_H}{Eu_G}}\left(\frac{1}{\eta}\sqrt{\frac{C_H}{Eu_G}} + 1\right) gH}{N_p \rho (ND)^2 gH}$$

$$= C_H \frac{\left(\frac{1}{\eta}\frac{C_H}{Eu_G} + \sqrt{\frac{C_H}{Eu_G}}\right)}{N_p \rho g H} \qquad (22)$$

Now the sought for optimality criterion or the aerator performance index can be obtained:

$$\frac{Q_G H}{P} = \frac{C_H}{N_p \rho g}\left(\frac{1}{\eta}\frac{C_H}{Eu_G} + \sqrt{\frac{C_H}{Eu_G}}\right) \qquad (23)$$

Equation (23), when supplemented with an experimental plot of Eu_G against C_H, contains all that is necessary for modeling of self-inducting aerators. It contains no tank geometry terms. Consequently, the aerator performance at constant submergence should be essentially the same in tanks of different geometry and volume as long as η is a constant and there is no gas-liquid dispersion recirculation through the lower (inlet) part of the aerator, the rate of recirculation being affected by the tank walls and bottom closeness to the aerator.

Although a small variation in η with D/T ratio was observed (Cooper and Wolf, 1968; Hicks et al., 1976), it could be the result of the different measurement methods used. In the present study, aerator dimensionless pumping capacity η was found reasonably constant using an indirect method of gas capacity measurement. The value of η can be obtained in principle from only one experiment with arbitrary values of aerator diameter D and submergence H over the appropriate range of impeller rotational speed N. The experiments would determine the power input P and aerator gas capacity Q_G as a function of rotational speed N and in addition the power number N_p which in the case of self-inducting aerator is unlikely to be available from the literature.* The interval for N should be chosen to include the value which yields the maximum value for the ratio Q_G/P. The only adjustable parameter, the aerator's dimensionless pumping capacity η, can be easily determined by introducing the experimental data into Equation (23).

EXPERIMENTAL APPARATUS AND PROCEDURE

The pilot scale apparatus, schematically drawn in Figure 4, allowed the simultaneous measurement of the volumetric gas aspiration rate Q_G, the mechanical agitation power consumption P, impeller rotational speed N, and the air pressure H_2 above the liquid surface in the vessel. Visual observation of the process was possible. The apparatus consisted of a transparent cylindrical baffled vessel (to eliminate vortex) of the diameter 0.4 and height 0.6 m with a pressurized cover and changeable rotor/stator/standpipe assemblies of different designs. Air aspirated from the atmosphere was measured at the vessel outlet

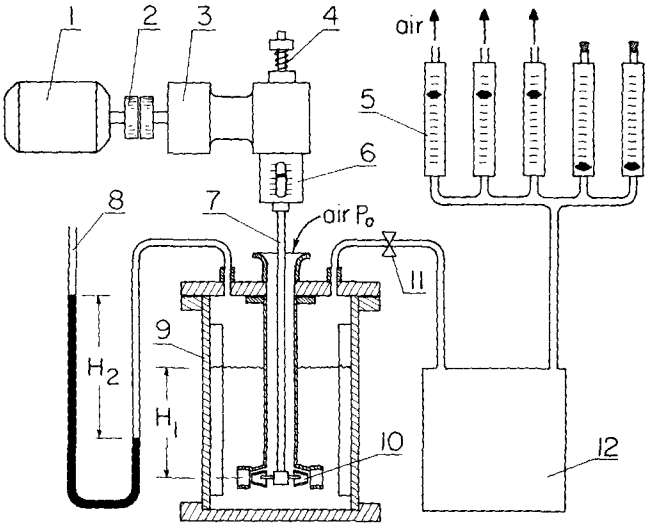

Fig. 4. Schematic diagram of apparatus: (1) variable speed motor, (2) shaft coupling, (3) gear box, (4) torsion spring, (5) air flowmeters, (6) torque meter, (7) shaft, (8) U shaped manometer, (9) tank, (10) aerating device, (11) control valve, (12) air receiver.

by means of a set of flowmeters. Five flowmeters, each with a range of 0.14 to 1.14 $\times$ 10^{-3}m^3/s, were used in combination as required to measure the flow with an accuracy of $\pm$2.5%.

By turning the control valve at the outlet, the air pressure H_2 above the liquid surface in the vessel could be increased to simulate submergence of the aerator up to 2.5 m of water. This excessive pressure was measured with a 2.5 m high U tube filled with water. Therefore, in the experiments described submergence H was equal to the sum of both air (H_2) and water (H_1) pressures, and absolute error of measurement did not exceed 2 to 3 $\times$ 10^{-2}m of water (clearly $H_2 = O$ and $H_1 = H$ under normal industrial conditions).

The aerator was actuated by variable geared motor drive (P = 1 500 W, N = 5 to 50 l/s); aerator shaft rotational speed was continuously measured by an optical tachometer device connected to a read-out indicator. Relative error of rotational speed measurement would not exceed 1.5%.

Torque measurements were carried out continuously during the experiment by means of a mechanical torque indicator. Maximum relative error of torque measurements was equal to 2.5%. Hence, the maximum relative error of power input determination was equal to the sum of both torque and rotational speed measurements errors and would not exceed 4.0%.

Measurement of the outlet air flow has advantages over the more usual measurement of the inlet (aspirated) air flow (Medvedev, 1955; Samsonova et al, 1970); these are:

1. No necessity to compensate for the pressure losses (head drop) at the aerator inlet due to resistances in the flowmeters and pipeline.
2. No necessity of shaft stuffing and as a result higher accuracy of the torque measurement.

EXPERIMENTAL RESULTS AND DISCUSSION

The goal of this paper is the development of general modeling principles rather than the description of the development of an optimal aerator design. Consequently, the experimental results are confined to only two aerator designs. The specifications are presented in Table 1.

Figures 5 and 6 give an example of the raw data obtained from the results of pilot scale experiments. These results were obtained using the aerator design (a) (Table 1). In Figure 7, the generalization of the experimental data from Figure 5 is shown in the form of the plot Eu_G against C_H [curve (a)]. The other curve (b) on the same figure shows the results of analogous processing of the experimental data obtained for aerator design (b) (Table 1). It is seen from Figure 7 that although different

* The value of N_p is calculated from Equation (16) on the basis of the experiment with no gas aspiration.

TABLE 1. AERATOR GEOMETRIES

(see Figures 2 and 3)

	D/T	d	D_0	D_s	h_0	h	h_s	Z	Z_s	α
Design (a)	0.25	$0.5D$	$0.6D$	$1.4D$	$0.22D$	$0.1D$	$0.2D$	6	12	30 deg
Design (b)	0.20, 0.25, 0.30	$0.67D$	$0.5D$	$1.25D$	$0.24D$	$0.12D$	$0.12D$	8	12	30 deg

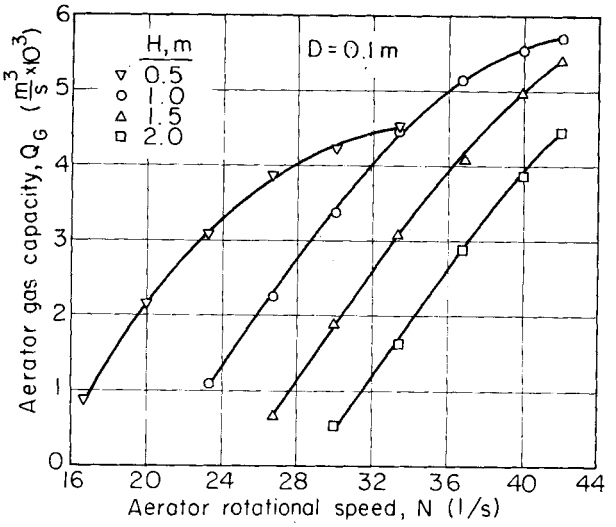

Fig. 5. Dependence of aerator gas capacity on aerator rotational speed for aerator rotor diameter 0.1 m [design (a)].

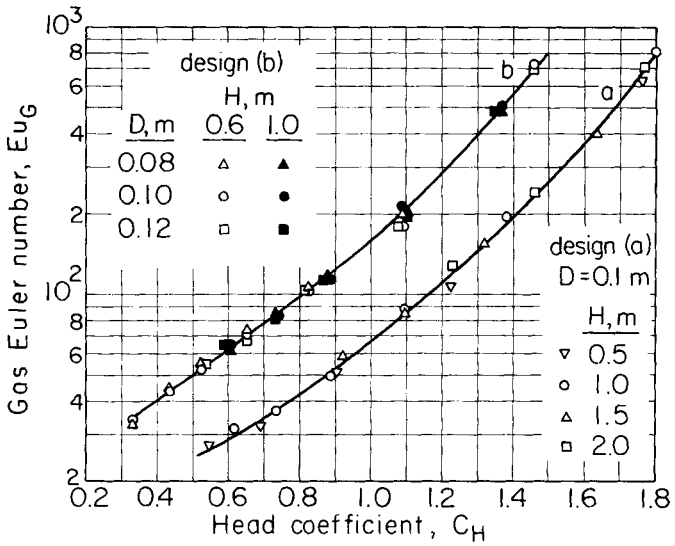

Fig. 7. Plot of gas Euler number against head coefficient for aerator designs (a) and (b).

values of submergence and aerator diameter were used in the experiments, the plots $Eu_G - C_H$ are the same for geometrically similar aerators. It is seen also that aerator design (a) (lower curve) is more efficient (in the sense of gas capacity) than aerator design (b) because for the same value of C_H the lower value of Eu_G corresponds to the higher gas rate [see Equation (20)].

For geometrically similar aerators, the single valued dependence exists between Eu_G and C_H. Therefore, it is easy to show that for constant values of aerator tangential velocity $U = \pi DN$ and submergence H (which implies that both Eu_G and C_H are constant), Equations (20) and (21) reveal the same dependence of gas capacity and power consumption on aerator diameter D: $Q_G \propto D^2$ and $P \propto D^2$. Consequently, their ratio Q_G/P is a constant value.

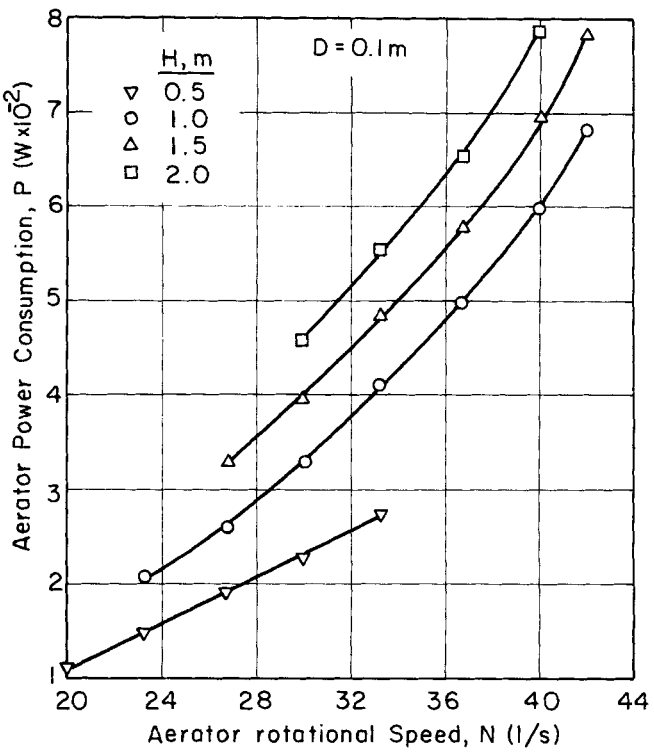

Fig. 6. Dependence of aerator power consumption on aerator rotational speed for aerator rotor diameter 0.1 m [design (a)].

A plot of the experimental data for design (b) according to Equations (20) and (21) is presented in Figures 8 and 9. The points on each curve represent the results of experimental determination of Q_G and P for three aerator diameters 0.08, 0.1, and 0.12 m [design (b), Table 1] at constant values of U and H. It is seen from Figures 8 and 9 that the experimental data conform to Equations (20) and (21).

It should be pointed out that this result is not for complete geometrical similarity (which includes the tank geometry) but rather for aerator similarity only. If full geometrical similarity were maintained, the value of H would increase proportionally to both aerator D and tank T diameters. Suppose the scale-up takes place on the basis of constancy of aerator performance index $Q_G H/P$ (if its value corresponds to the maximum, the optimal case obtains), that is, at the constant C_H and Eu_G. It is obvious that ratio $Q_G/P \propto 1/H$, that is, inversely proportional to the linear tank dimensions, as a result of the constancy of $Q_G H/P$.

Furthermore, aerator capacity Q_G, as it follows from Equation (20), increases as $Q_G \propto T^{5/2}$ (due to geometrical similarity: $D \propto H \propto T$). Power increases as $P \propto T^{7/2}$ [considering Equation (21) and the obvious relationship $ND \propto H^{1/2} \propto T^{1/2}$, following from C_H being a constant]. Finally, the tank volume and horizontal cross section are, respectively, $V \propto T^3$ and $A \propto T^2$. Consequently, both superficial velocity $U_s = Q_G/A \propto T^{5/2}/T^2 = T^{1/2}$ and power per unit of volume $P/V \propto T^{7/2}/T^3 = T^{1/2}$ must increase as the square root of linear dimension. It is clear that com-

TABLE 2. PROPERTIES OF TANK WITH SELF-INDUCTING AERATOR ON SCALE-UP (Q_GH/P, C_H, Eu_G = CONST)

	Geometrical similarity			
	Complete	Partial		
	$T \propto H \propto H_L \propto D$	$T \propto H \propto H_L$, U_s = const	$T \propto D \propto H_L$, U_s, H = const	$T \propto D$, U_s, H, H_L = const
1	2	3	4	5
Property	Property variation with tank diameter			
H	T	T	const	const
D	T	$T^{3/4}$	T	T
U_s	$T^{1/2}$	const	const	const
D/T	const	$T^{-1/4}$	const	const
N	$T^{-1/2}$	$T^{-1/4}$	T^{-1}	T^{-1}
ND	$T^{1/2}$	$T^{1/2}$	const	const
V	T^3	T^3	T^3	T^2
Q_G	$T^{5/2}$	T^2	T^2	T^2
P	$T^{7/2}$	T^3	T^2	T^2
P/V	$T^{1/2}$	const	T^{-1}	const
Q_G/P	T^{-1}	T^{-1}	const	const
Q_G/V	$T^{-1/2}$	T^{-1}	T^{-1}	const
Q_G/ND^3	const	const	const	const

plete geometrical similarity appears to be contrary to kinematic and energetic similarity. Proceeding this way, the large variety of analogous relationships between the properties relevant to dimensions, velocities, or fluid forces and the tank diameter can be obtained for complete as well as for partial geometrical similarity (Table 2). It is seen from Table 2 that complete geometrical similarity (column 2) appears to be less economical on scale-up, whereas partial geometrical similarity (columns 3 to 5) give more acceptable engineering solutions. Table 2 may serve as a guide in choosing the scale-up strategy if for some reason geometrical similarity is required. The most flexible solution obtains, however, when aerator and tank characteristics are determined without prescribing a specific geometrical correlation between them.

So the plots of Eu_G against C_H and aerator performance index Q_GH/P are the main characteristics of a self-inducting aerator of any particular design. For aerator design (a), the values of power number N_p and dimensionless pumping capacity η were determined to be equal to 3.1 and 0.071, respectively, by processing the results of experiments. The value of Q_GH/P was computed for the entire range of C_H values, using Equation (23) and the plot of Eu_G against C_H (Figure 7, curve a). The results of computation (broken line) and processed experimental data from Figures 5 and 6 (solid line) are shown in Figure 10. The two curves are very close to each other and coincide in the vicinity of maximum, in practice the most important region. The maximum for this case corresponds to $C_H = 0.9$. The value of Eu_G corresponding to $C_H = 0.9$ is $Eu_G = 53$ (Figure 7, curve a). The maximum value of Q_GH/P on Figure 10 equals 1.08×10^{-5} m^4/W·s.

Figure 11 provides an analogous comparison of computed and experimentally obtained plots for aerator design (b), where three geometrically similar aerators were investigated (see, also, Figure 7, curve b), the values of N_p and η being equal to 2.5 and 0.048, respectively. It is seen from Figure 11 that there is a single valued dependence of Q_GH/P on C_H for the variety of combinations H and D. The superiority of aerator design (a) over design

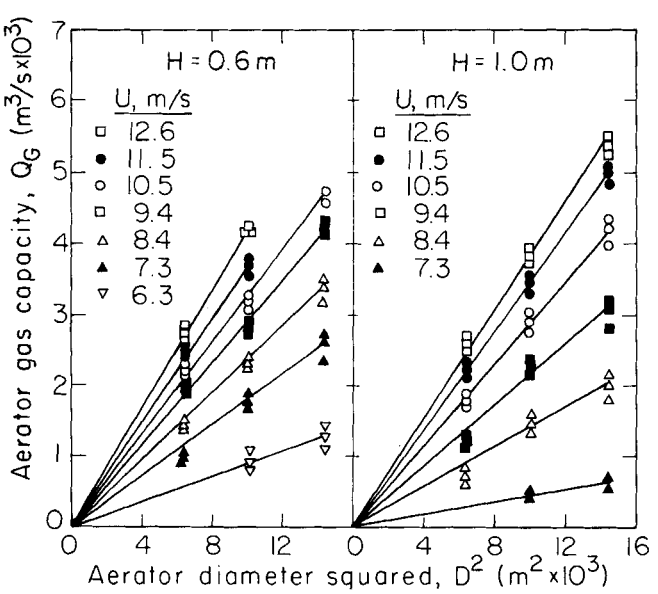

Fig. 8. Dependence of aerator gas capacity on aerator diameter when rotor tip speed and aerator submergence are constant [design (b)].

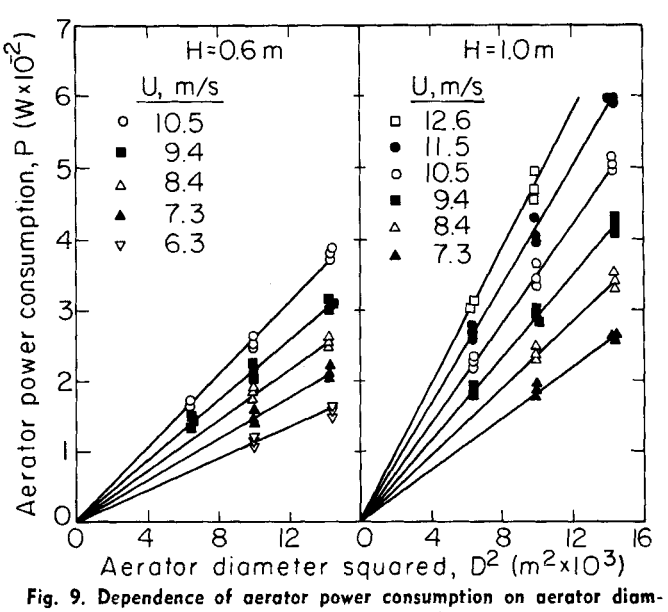

Fig. 9. Dependence of aerator power consumption on aerator diameter when rotor tip speed and aerator submergence are constant [design (b)].

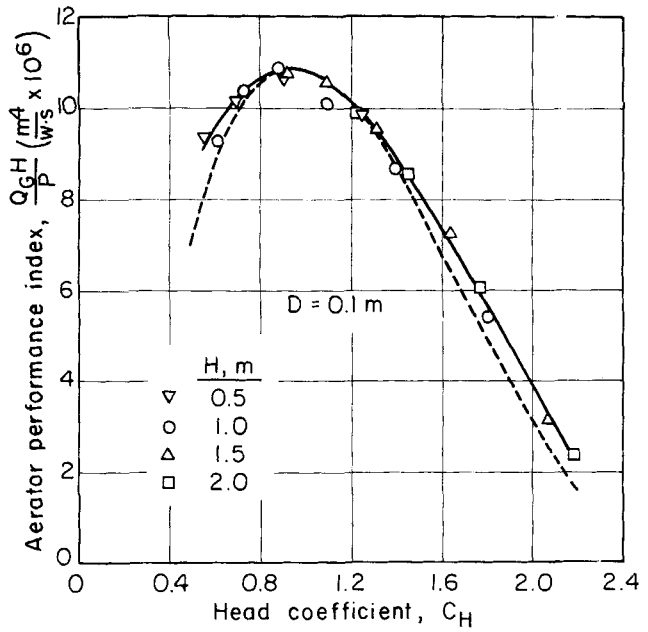

Fig. 10. Variation of aerator performance index computed from Equation (23) (broken line) and analogous value obtained as a result of processing the experimental data from Figures 5 and 6 (solid line) with head coefficient [design (a)].

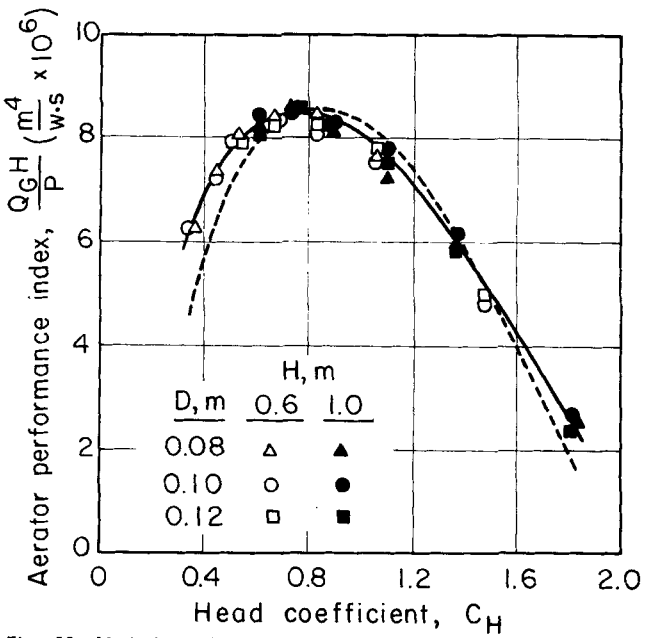

Fig. 11. Variation of aerator performance index computed from Equation (23) (broken line) and analogous value obtained as a result of processing the experimental data from Figures 8 and 9 (solid line) with head coefficient [design (b)].

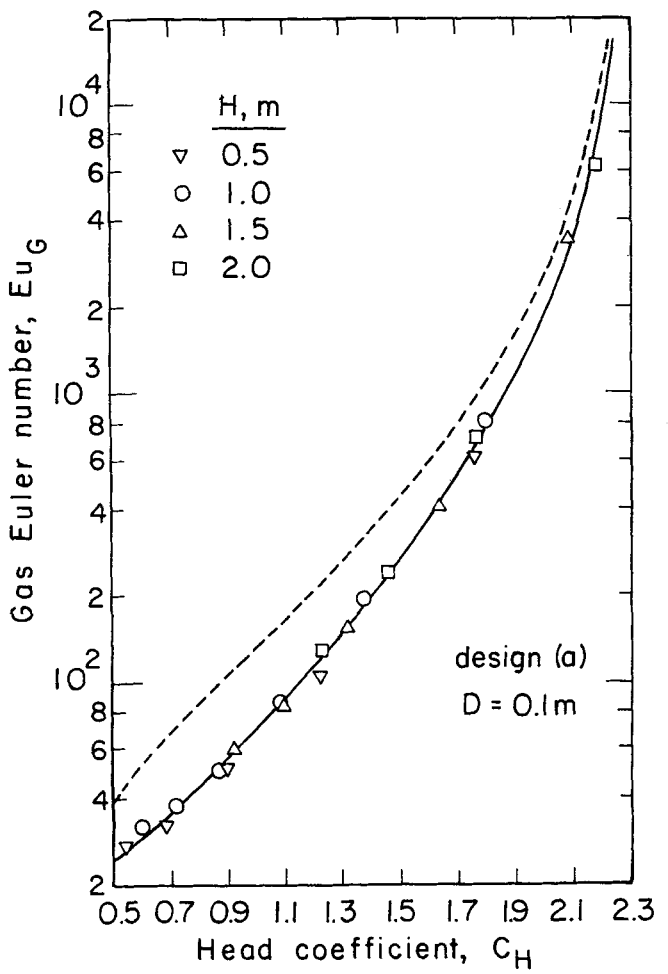

Fig. 12. Comparison of the plot for gas Euler number against head coefficient computed from Equation (13) (broken line) with analogous plot from Figure 7 (solid line). Design (a).

(b) is immediately apparent in a comparison of Figures 10 and 11; the maximum value of aerator performance index of design (a) is substantially higher than that of design (b). In addition, the former exhibits a shift to the right with respect to design (b). This means that maximum performance for design (a) is achieved at lower rotor speed.

Although rotor diameter D was varied only 1.5 fold (due to the very strong affect on both P and Q_G), the submergence H (which also strongly influenced P and Q_G) was varied over a wide interval which covers most of the real industrial applications. It is expected, therefore, that Figures 10 and 11 apply to other geometrically similar aerators due to a singular dependence between Eu_G and C_H [Equation (13)], coefficients K_1, and η being reliably stated as constants.

Figures 7 and 10 can be used by the designer to calculate the optimal aerator design. The optimal design procedure is as follows:

1. Power requirement should be determined from $Q_G H/P = 1.08 \times 10^{-5}$ m^4/W·s on the basis of values of Q_G and H assigned.

2. Aerator diameter should be determined from the value of $Eu_G = 53$

$$D = \sqrt[4]{\frac{Q_G^2 Eu_G}{gH}}$$

3. Aerator rotational speed is determined from the value of $C_H = 0.9$, using the above value for D

$$N = \sqrt{\frac{gH}{D^2 C_H}}$$

In particular, $N = N_{cr}$ obtains when the numerical value of C_H in the latter expression corresponds to the beginning of gas inducing [compare to Equation (1)].

It is worthwhile to compare the experimental results with Equation (13), which gives the relation between Eu_G and C_H based on the characteristics of water jet injectors. To obtain the plot of Eu_G against C_H and compare the latter with the experimentally obtained one (Figure

7), it is necessary to define the coefficient K_1 in Equation (13). This is readily achieved using Equation (10) for the injection coefficient under the condition $\Psi = 0$, that is, when the aerator is just about to start gas aspiration. The value of C_H for aerator design (a) corresponding to this condition was found to equal 2.35 experimentally. Substituting this value into Equation (10) at $\Psi = 0$, we get $K_1 = 1.15$. Then, using Equations (10) and (13), it is possible to compute values of Eu_G for the several values of C_H taken from the same range as in Figure 7.

The results of the comparison of computed (broken line) and experimentally obtained (solid line) plots of Eu_G against C_H are shown in Figure 12. The discrepancy between the curves, surprisingly, turned out to be not very great, taking into account the use of constants in Equation (3) which were originally determined for water jet injectors and the high degree of arbitrariness in stating the equivalence of injector and aerator geometry elements to be used in Equation (3). The same reasons may explain why the coefficient K_1 is greater than unity which is nonphysical.

Nevertheless, the shapes of the curves on Figure 12 seem to be very similar, which supports the approach of this study, that self-inducting aerators can be successfully modeled by exploiting their similarity to water jet injectors.

ACKNOWLEDGMENT

E. Vigdorchik (Laboratory of Mathematical Modeling of Metallurgical Processes of Research and Design Institute Gipronickel, Leningrad, U.S.S.R.) provided valuable suggestions regarding representation of the experimental results. The author also wishes to thank J. W. Evans for constructive reviewing of the manuscript.

NOTATION

A = horizontal cross-sectional area of the tank, m^2
D = aerator's rotor diameter, m
D_s = aerator's stator diameter, m
C_H = head coefficient, $gH/(ND)^2$, dimensionless
Eu_G = gas Euler number, $gH/(Q_G/D^2)^2$, dimensionless
g = gravitational acceleration, m/s^2
h = rotor blade width, m
h_s = stator blade width, m
H_L = liquid fill height of tank, m
H = aerator submergence, m
H_2 = excess pressure above liquid surface in the experimental vessel, m
H_1 = liquid height above aerator in the experimental vessel, m
K = driving medium velocity coefficient in Equation (3), dimensionless
K_1 = coefficient of head losses in aerator, dimensionless
N_p = power number, $P/\rho N^3D^5$, dimensionless
N = aerator rotational speed, s^{-1}
N_{cr} = critical aerator speed (beginning of gas inducing), s^{-1}
P = mechanical agitation power, W
p_s = static head of rotor, Kg/m·s^2
p_M = pressure of the outer medium (at the injector outlet), Kg/m·s^2
p_N = pressure of the working liquid (at the nozzle outlet), Kg/m·s^2
p_0 = gas pressure at the injector inlet, Kg/m·s^2
$\Delta p_M = p_M - p_0$, injector pressure differential, Kg/m·s^2
$\Delta p_N = p_N - p_0$, nozzle pressure differential, Kg/m·s^2
Q_G = aerator gas capacity, m^3/s
S_N = cross-sectional area of the nozzle, m^2
S_M = cross-sectional area of the mixing chamber, m^2
Q_L = impeller pumping capacity, m^3/s
T = tank diameter, m
U = aerator tangential velocity, m/s
$U_s = Q_G/A$, superficial velocity, m/s
V = tank volume, m^3
Z = rotor blades number, dimensionless
Z_s = stator blades number, dimensionless

Greek Letters

α = angle between radius and stator blade, deg
$\eta = Q_L/ND^3$, dimensionless impeller pumping capacity
ρ = liquid density, Kg/m^3
ρ_D = gas-liquid dispersion density, Kg/m^3
ρ_G = gas density, Kg/m^3
σ = gas-liquid surface tension, N/m
ζ_1 = nozzle velocity coefficient in Equation (3), dimensionless
ζ_2 = diffusor velocity coefficient in Equation (3), dimensionless
$\Psi = Q_G/Q_L$, dimensionless

LITERATURE CITED

Arbiter, N., C. C. Harris, and R. Yap, "A Hydrodynamic Approach to Flotation Scale-up," Preprint D-19:12, 8th Mineral Processing Congress, Institute Mekhanobre, Leningrad, Russia (1968).

Blakebrough, N., and K. Sambamurthy, "Performance of Turbine Impellers in Sparger-Aerated Fermentation Vessels," *J. Appl. Chem.*, **14**, 413 (1964).

Braginsky, L. N., "The Study of Aeration Characteristics of Impellers for Autoclave Leaching Processes," Scientific Report on Research Project, Research and Design Institute NIIKhIMMASH, Leningrad, Russia (1964).

Bruijn, W., K. Van't Riet, and J. M. Smith, "Power Consumption with Aerated Rushton Turbines," *Trans. Inst. Chem. Engrs.*, **52**, 88 (1974).

Calderbank, P. H., "Physical Rate Processes in Industrial Fermentation, Part I: The Interfacial Area in Gas-Liquid Contacting with Mechanical Agitation," *ibid.*, **36**, 443 (1958).

———, "Physical Rate Processes in Industrial Fermentation. Part II: Mass Transfer Coefficients in Gas-Liquid Contacting with and without Mechanical Agitation," *ibid.*, **37**, 173 (1959).

———, and M. Moo-Young, "The Continuous Phase Heat and Mass Transfer Properties of Dispersions," *Chem. Eng. Sci.*, **16**, 39 (1961).

Cooper, R. G., and D. Wolf, "Velocity Profiles and Pumping Capacities for Turbine Type Impellers," *Can. J. Chem. Eng.*, **46**, 94 (1968).

Fort, I., "Studies on Mixing. Part 24. Pumping Capacity of Propeller Mixer (Analytical Study)," *Collect. Czechosl Chem. Communs.*, **34**, 1094 (1969).

Harris, C. C., "Flotation Machines," *Flotation*, A. M. Gaudin Memorial Edition, Vol. 2, pp. 753-815, AIME (1976).

Hassan, I. T. M., and C. W. Robinson, "Stirred-Tank Mechanical Power Requirement and Gas Holdup in Aerated Aqueous Phases," *AIChE J.*, **23**, 56 (1977).

Hicks, R. W., J. R. Morton, and J. G. Fenic, "How to Design Agitators for Desired Process Response," *Chem. Eng.*, 104 (Apr. 26, 1976).

Joshi, J. B., and M. M. Sharma, "Mass Transfer and Hydrodynamic Characteristics of Gas Inducing Type of Agitated Contactors," *Can. J. Chem. Eng.*, **55**, 683 (1977).

Kashkarov, I. F., "Some Conditions Governing the Work of Mechanical Flotation Machines having Centrifugal Impellers," Ordzhonikidze (1956).

Klassen, V. I., "The Problems of Aeration and Flotation Theory," Goskhimizdat, Moscow, 1949.

———, "On Coals Flotation," Ugletekhizdat (1954).

Lee, J. C., and D. L. Meyrick, "Gas-Liquid Interfacial Areas in Salt Solutions in an Agitated Tank," *Trans. Inst. Chem. Engrs.*, **48**, T37 (1970).

Medvedev, S. A., "The Control of Flotation Machine Performance with Respect to Air Consumption," Ugletekhizdat (1955).
———, and L. Ya Shestakov, "The Testing of Mechanical Flotation Machines," Tsiin, Moscow, Russia (1957).
Michel, B. J., and S. A. Miller, "Power Requirements of Gas-Liquid Agitated Systems," *AIChE J.*, **8**, 262 (1962).
Mitrofanov, S. I., "The Concentration of Non-Ferrous Metals Ores," *The Proceedings of Niitsvetmet*, Issue 16, Moscow, Russia (1959).
———, "Selective Flotation," Nedra, Moscow, Russia (1967).
Oyama, Y., and K. Endoh, "Power Characteristics of Gas-Liquid Contacting Mixers," *Chem. Eng. (Tokyo)*, **19**, 2 (1955).
Robinson, C. W., and C. R. Wilke, "Oxygen Absorption in Stirred Tanks: A Correlation for Ionic Strength Effects," *Biotechnol. Bioeng.*, **15**, 755 (1973).
Rundkvist, V. A., "The Study of Performance of Self-Inducting Impellers Designed by Mekhanobre. Part 1," *Concentration of Ores*, issue 5 (1963).
———, "The Study of Performance of Self-Inducting Impellers Designed by Mekhanobre. Part 2," *ibid.*, issue 1 (1964).
Samsonova, A. F., V. M. Khudiakov, and G. N. Dobrokhotov, "Testing of Self-Inducting Device with Upper Drive for the Autoclave #2 at the Plant Yuzhuralnickel," *The Proceeding of Gipronickel*, issue 49, 103 (1970).
Sokolov, E. Ya., and N. M. Zinger, "The Jet Devices," Moscow, Gosenergoizdat (1960).
Topiwala, H. H., and G. Hamer, "Mass Transfer and Dispersion Properties in a Fermenter with a Gas-Inducing Impeller," *Trans. Inst. Chem. Engrs.*, **52**, 113 (1974).
Uhl, V. W., and J. B. Gray, *Mixing—Theory and Practice*, Vol. 1, Academic Press, New York (1966).
Van't Riet, K., J. M. Boom, and J. M. Smith, "Power Consumption, Impeller Coalescence and Recirculation in Aerated Vessels," *Trans. Inst. Chem. Engrs.*, **54**, 124 (1976).
Zaytsev, V. A., "Study of Effect of Self-Inducting Aerator Geometry on Aeration Characteristics of Tanks," *Theory and Practice of Stirring in Liquid Media*, NIITEKhIM, Moscow, Russia (1973).
Zundelevich, Y. V., "Development of Self-Inducting Aerator for Norilsk Plant Autoclaves," Technical Report on Research Project, Research and Design Institute Gipronickel, Leningrad, Russia (1975).

Manuscript received June 30, 1978; revision received February 22, and accepted April 18, 1979.

On the Kinetics of Coal Oxidation

N. L. AVISON
R. M. WINTERS
and
D. D. PERLMUTTER

Department of Chemical and Biochemical Engineering
University of Pennsylvania
Philadelphia, Pennsylvania 19104

A series of seven coals of different ranks and from various locations were heated in air under relatively mild conditions to measure the rates of oxidation and the production of carbonic gases in the effluent stream. The gas flow rate, coal particle size, and reactor temperature were changed as independent variables. Each sample was exposed for from 6 to 9 hr under atmospheric pressure at temperatures in the range of 200° to 250°C. The results show two kinds of rate behavior depending primarily on the relative porosity of the coal under study. The small pore coals followed the expectations of the earlier Kam-Hixson-Perlmutter (KHP) model, but the large pore coals gave rates sensitive to transport effects. Correlations were also obtained on the ratio of carbon dioxide and carbon monoxide produced and on the relationship between the carbon content of an exposed coal and its heating value.

SCOPE

The rates at which a variety of coals undergo mild gas phase oxidation were measured in a fixed-bed reactor under a range of flow rates and for various particle sizes. Seven coals from different sources were tested at three temperatures. The coals pretreated in this manner were analyzed for chemical composition and heating value changes, and the oxidation off-gases were analyzed for carbonic gas content. Correlations were prepared in terms of an earlier KHP model and exceptional behavior noted for specific coals.

CONCLUSIONS AND SIGNIFICANCE

As a result of experimental oxidation tests on seven coals from different sources, it has been found that not one but two models are needed to distinguish between large and small pore coals. The earlier KHP model, which was based on the expectation of very small diffusion rates for gases into coal, remains valid for the largest group of coals tested but has to be modified for at least two of the coals. When the coals had relatively large pore volumes in the size range greater than 300Å, the oxidation rate was found to be sensitive to particle size, gas flow rate, and reaction temperature, in a manner indicating significant transport effects. Correlations of the carbon dioxide to carbon monoxide ratio obtained from runs under varying conditions also support the applicability of the KHP model. The heating values among the various coal samples changed upon oxidation in a manner dependent primarily on the changes in carbon content of the coal.

N. L. Avison is with Mobil Research and Development Corporation, Paulsboro, New Jersey 08066. R. M. Winters is with Air Products and Chemicals, Inc., Allentown, Pennsylvania 18105.

0001-1541-79-2595-0772-$01.05.